Effect of Misalignment of Inductive Wireless Power Transfer Coils

Christopher Mullen[1, 2], Soobum Lee[2]
[1]U.S. Army Combat Capabilities Development Command (DEVCOM), C5ISR Center, RTI, Power Division
Aberdeen Proving Ground, MD 21005, USA
[2]Department of Mechanical Engineering, University of Maryland, Baltimore County
214 Engineering Building, 1000 Hilltop Circle, Baltimore, MD 21250

Abstract

As inductive wireless power transfer becomes ubiquitous for charging phones and other portable electronics, consumers are less worried about efficiency and more concerned with high charging rates. For a Soldier in the field, less efficiency means they must carry more batteries or fuel, or forgo wireless charging altogether. To determine changes in wireless power transfer efficiency with respect to inductor misalignment, this research develops the equations used to calculate inductance, mutual inductance, and coupling coefficient depending on inductor geometry and distance. The results show that despite inductive coils that are not well coupled, there are strategies to maintain the same power transfer efficiency as perfectly coupled coils.

Keywords

Wireless power transfer; Inductive power transfer; Charging efficiency; Coil misalignment

Introduction

Wireless power transfer (WPT) was introduced by Tesla over one hundred years ago, yet researchers are still peeling back the layers to fully understand the ways we can take advantage of this powerful technology. WPT includes any technology that sends power without being directly connected via wires or cables, from two capacitive plates to an antenna via radio frequency (RF) [1]. Inductive wireless power transfer (IWPT) uses concepts from electrodynamics, specifically Maxwell's equations, whereby an alternating electric current that flows through a wire will produce a magnetic field around the wire. The magnetic field can be described mathematically through the relationship between current density, magnetic field intensity, and material permeability. Current density (J) through the wire is equal to the curl of the magnetic field intensity (H), and the field intensity times material permeability (μ) is equal to the magnetic field (B), sometimes referred to as magnetic flux density [2]. When current flows through a wire, the magnetic field flows around the wire and interacts with its environment. If a second wire is placed within the magnetic field produced by the first wire, that alternating magnetic field will induce an electrical current in the second wire as described by Faraday's Law of electromagnetic induction. The wire is an inductor, and how to optimize the inductor for efficient WPT is the focus of this research.

The quality factor (Q) is the ratio of the reactance to the resistance of the inductor, and as the quality factor increases, so does the power transfer efficiency [3]. For WPT it is important that the wire transmitting power minimizes its resistance and maximizes its inductance, and previous studies have focused on how to create different topologies with the wire that will optimize its quality factor [4]. This paper will focus on circular coil inductors. Quality factor increases proportionately to coil inductance and frequency, and is inversely proportional to coil resistance.

As the secondary coil moves with respect to the primary coil, the change will be reflected in the coupling coefficient (k). As equations have been developed to derive the coupling coefficient, they have customized the Neumann integral to fit coils with rectangular and circular cross-sections. However, only the basic calculation is shown while misalignment of the coils is not generally derived [5]. The coupling coefficient is a measure of how efficiently the primary coil is sending power to the secondary coil, and is calculated by dividing the mutual inductance (M) which is the square root of the product of the two inductors (L1 and L2). When the two coils are perfectly coupled, the coefficient approaches 1.0. Previous papers have manipulated the Neumann integral to show the change in mutual inductance and the coupling coefficient as the secondary coil is displaced with respect to the primary coil [6-7]. This paper will focus on the agreement between the accuracy of the model when compared to experimental results, and will highlight changes in efficiencies with respect to misalignment.

Method of Determining Coupling Coefficient

The Neumann integral is used to calculate the mutual inductance as shown in Equation 1:

$$M_{12} = \frac{\mu 0}{4\pi} \oint \oint \frac{dl1 \cdot dl2}{R_{QN}} \tag{1}$$

The variable μ_0 is the permeability of free space, R_{QN} is the distance between the two differential arc lengths, and defined in Equation 1. R_{QN} can be derived from the Pythagorean Theorem [5].

$$R_{QN} = \sqrt{r_1^2 + r_2^2 + d^2 - 2r_1 r_2 \cos\phi} \tag{2}$$

The variables r_1, r_2, d, and ϕ are defined as the primary coil radius, secondary coil radius, distance between the center of both coils, and the angle defined to indicate the location of the infinitesimal direction vector at each coil: $d\boldsymbol{l}_1$ and $d\boldsymbol{l}_2$, respectively.

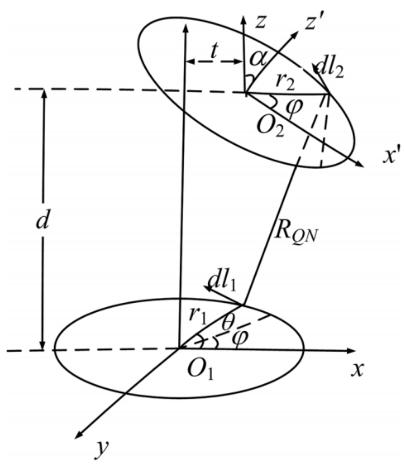

FIG. 1 Two coils separated by distance, *d* [6].

This derivation only takes into consideration a single degree of freedom in the *z*-direction, defined by the distance variable, d. By expanding Equation 1, this paper derives the equations for displacement of the secondary coil in the *x* and *y* direction as well as rotation about the *x* and *y*-axes (φ, α). The dot product between $d\boldsymbol{l}_1$ and $d\boldsymbol{l}_2$ can be rewritten using the radius of each coil along with the angle parameters.

$$dl_1 \cdot dl_2 = r_1 r_2 (cos\,\phi_1\,cos\,\phi_2\,cos\,\alpha + sin\,\phi_1\,sin\,\phi_2 \quad (3)$$

$$R_{QN} = \sqrt{\begin{array}{l}(x + r_2\,cos\,\phi_2\,cos\,\alpha - r_1\,cos\,\phi_1)^2 \\ +(y + r_2\,sin\,\phi_2 - r_1\,sin\,\phi_1)^2 \\ +(d - r_2\,cos\,\phi_2\,sin\,\alpha)^2\end{array}} \quad (4)$$

In Equation 4, the distance (*d*) is simulated by adding the experimental distance between the coils plus half the thickness in the *z*-direction of each coil, so that if both the coils are 1 mm thick, and the experimental distance between the coils is 3 mm, then the simulated distance is 4 mm. When there is no displacement in the *x* and *y* directions and no rotation about the *y*-axis, Equation 4 simplifies to Equation 2. Equation 5 is the result of multiplying out Equation 4, which helps to avoid infinite results when solving the equation.

$$R_{QN} = \sqrt{\begin{array}{l}x^2 + y^2 + d^2 + r_1^2(cos^2\,\phi_1 + sin^2\,\phi_1) \\ +r_2^2(cos^2\,\phi_2\,cos^2\,\alpha + sin^2\,\phi_2 + cos\,\phi_2\,sin\,\alpha) \\ +r_1(2c\,cos\,\phi_1 - 2g\,sin\,\phi_1) \\ +r_2(2c\,cos\,\phi_2\,cos\,\alpha + 2g\,sin\,\phi_2 - 2d\,cos\,\phi_2\,sin\,\alpha) \\ -2r_1r_2(cos\,\phi_1\,cos\,\phi_2\,cos\,\alpha + sin\,\phi_1\,sin\,\phi_2)\end{array}} \quad (5)$$

When multi-turn coils are considered (N_1, N_2), Equation 1 can be rewritten as:

$$M_{12} = N_1 N_2 r_1 r_2 \frac{\mu 0}{4\pi} \oint \oint \frac{cos\,\phi_1\,cos\,\phi_2\,cos\,\alpha + sin\,\phi_1\,sin\,\phi_2}{R_{QN}}\; d\phi_1 d\phi_2 \quad (6)$$

The self-inductance of the coils is derived using the Neumann integral. In this paper, instead of using the distance between two coils, we use the distance between the middle of the coil and the inside diameter of the same coil. For the self-inductance calculation, to take into consideration the interaction of the turns, we are multiplying by N^2 instead of multiplying N_1 and N_2.

$$L_1 = L_2 = \frac{N^2 r(r - r_w)\mu 0}{4\pi} \oint \oint \frac{cos(\phi_2 - \phi_1)}{R_d}\; d\phi_1 d\phi_2 \quad (7)$$

$$R_d = \sqrt{r^2 + (r - r_w)^2 - 2r(r - r_w)\,cos(\phi_2 - \phi_1)} \quad (8)$$

Now that both mutual inductance and self-inductance have been derived. Coupling coefficient is calculated by dividing mutual inductance by the square root of the product of L_1 and L_2.

$$k = \frac{M_{12}}{\sqrt{L_1 L_2}} \quad (9)$$

Method of Experimental Data Collection

The experiments were conducted at the Army Research Center in Adelphi, MD using a network analyzer. The equipment was first calibrated, then the inductors were attached to the network analyzer and placed at intervals ranging from 1mm to 5mm distance for the 10mm diameter multi-turn coils and from 0.25cm to 2cm distance for the 35mm diameter single turn coils. The coils were concentrically placed, and rubber stops were used to hold the inductors in place. Glass microscope slides, 1mm thick, were placed between the 10mm diameter inductors and measurements were taken and saved. For the 35mm diameter coils, glass objects were measured and placed between the inductors. The data was stored in the network analyzer and later transferred for analysis.

Results and Discussion

For the 35mm diameter single turn coils, the results are shown in Table 1 and Table 2 for the experimental and simulation results, respectively, and plotted in Figure 4.

TABLE 1: Experimental results from 35mm diameter single turn coils.

distance	0.25cm	0.5 cm	1 cm	2cm
k	0.3624	0.2956	0.1670	0.0672
L_1 (H)	1.3E-07	1.3E-07	1.3E-07	1.3E-07
L_2 (H)	1.2E-07	1.2E-07	1.2E-07	1.2E-07
M (H)	4.5E-08	3.6E-08	2.1E-08	8.3E-09
f (kHz)	103	103	103	103
R_1 (Ω)	0.0044	0.017	0.0131	0.0038
R_2 (Ω)	0.0159	0.007	0.0105	0.0096

TABLE 2: Simulation results from 35mm diameter single turn coils.

distance	0.25 cm	0.5 cm	1 cm	2cm
k	0.5615	0.3848	0.2226	0.0957
L_1 (H)	8.9E-08	8.9E-08	8.9E-08	8.9E-08
L_2 (H)	8.8E-08	8.8E-08	8.8E-08	8.8E-08
M (H)	5.0E-08	3.4E-08	2.0E-08	8.5E-09
f (kHz)	100	100	100	100

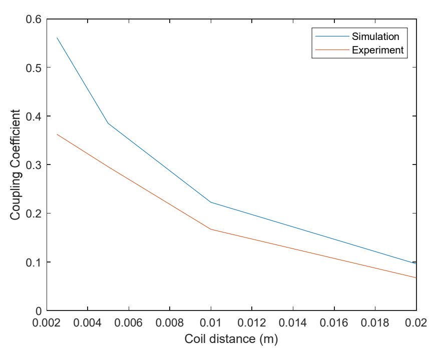

a)

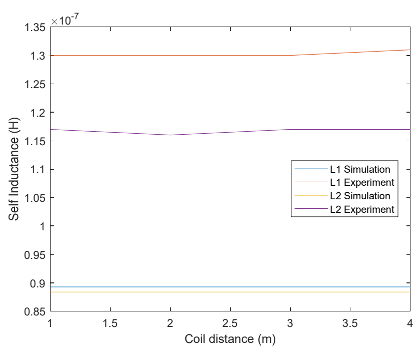

b)

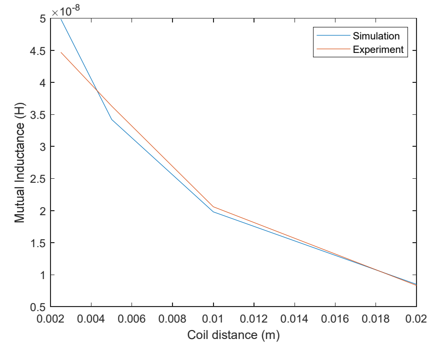

c)

FIG. 3: a) Coupling Coefficient results. b) Self-inductance results. c) Mutual inductance results.

As is typical with inductive power transfer systems, there is an exponential decay in the coupling coefficient as the distance of the concentric coils increases. There is good agreement between the experimental and simulated mutual inductances. The discrepancy in the coupling coefficient calculation comes from the self-inductance results, due to the length of the inductor leads and solder.

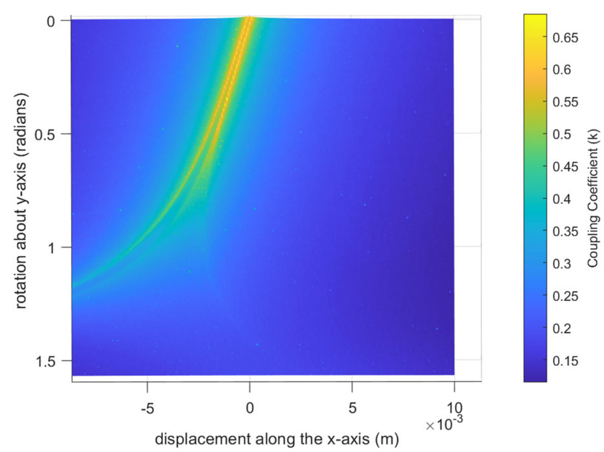

FIG. 4: Coupling coefficient with varying rotation about the y-axis and displacement along the x-axis.

The results of the simulation in Figure 4 show that the most reliable coupling coefficient for the 35 mm diameter coils can be found where the two coils are slightly rotated 0.064 radians when displaced 0.64 mm along the *x*-axis. Intuitively the maximum coupling coefficient is found when zero. The efficiency is well maintained along the path of the magnetic field, diminishing with increasing distance between the coils.

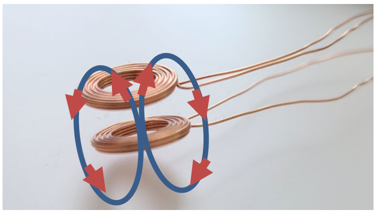

FIG. 5: Shape of the magnetic field from the primary coil.

As the magnetic field moves in a circular direction from "north" to "south", as in Figure 5, the displaced secondary coil can capture more of the field by increasing rotation about the x or y axes. The secondary coil will be more efficient if it is perpendicular to the direction of the magnetic field. This research quantifies what the angle α and φ of the secondary coil should be with respect to the primary coil given a distance (d) between the two coils that will maximize efficiency.

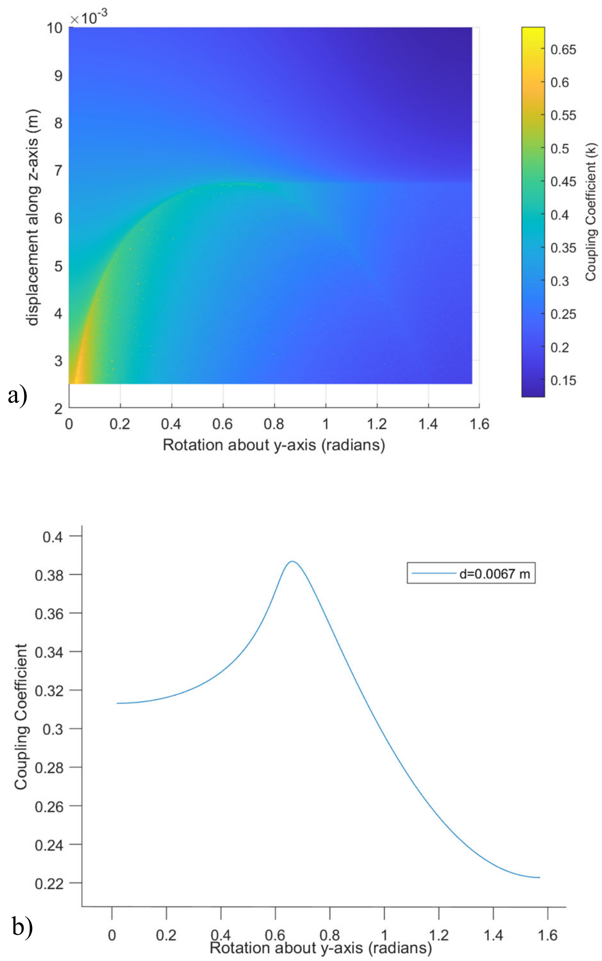

FIG. 6: (a) Coupling coefficient with varying rotation about the y-axis and displacement along the z-axis. (b) Fixed distance (d) with varying rotation about the y-axis.

Looking further at a different combination of alignment variables, Figure 6(a) illustrates the changing coupling coefficient by the change of displacement along the z-axis and rotation about the y-axis. The figure shows that as the distance between the coils increases, the optimal rotation of the secondary coil is non-zero due to the shape of the magnetic field. There is no data for a displacement up to 0.0025 m because of the insulation coating the copper inductor. Figure 6(b) holds constant displacement along the z-axis (d=0.0067 m) and increases rotation about the y-axis, essentially drawing a straight line from the left side of Figure 6(a) to the right side. Given the uncertainty of alignment in applications such as UAVs charging mid-flight and wearable wireless power transfer, this data can be added to a control algorithm for a UAV to maximize efficiency or explain why one set of data is performing better than another.

This research develops the equations used to calculate inductance, mutual inductance, and coupling coefficient depending on inductor geometry and coil misalignment, and uses that information to determine changes in efficiency with greater misalignment. The results show that although inductive coils might not be well coupled, there are strategies to maintain the same power transfer efficiency as perfectly coupled coils.

Acknowledgements

The authors wish to thank the In-House Laboratory Independent Research (ILIR) program for funding this research as part of an effort to optimize wireless power transfer.

References

1. Rim, Chun T., and Chris Mi. *Wireless power transfer for electric vehicles and mobile devices*. John Wiley & Sons, 2017.
2. Griffiths, David J. *Introduction to Electrodynamics Fourth Edition*. Prentice-Hall, 2021.
3. Lazarus, N., and S. S. Bedair. "Improved power transfer to wearable systems through stretchable magnetic composites." *Applied Physics A* 122 (2016): 1-7.
4. Yoo, Byungseok, et al. "Laser Direct Structured 3D Circuits on Silicone." *ACS Applied Materials & Interfaces* 14.16 (2022): 18854-18865.
5. Paul, Clayton R. *Inductance: loop and partial*. John Wiley & Sons, 2011.
6. Gao, Pengfei, et al. "Transmission efficiency analysis and optimization of magnetically coupled resonant wireless power transfer system with misalignments." *AIP Advances* 8.8 (2018): 085016.
7. Fotopoulou, Kyriaki, and Brian W. Flynn. "Wireless power transfer in loosely coupled links: Coil misalignment model." *IEEE Transactions on magnetics* 47.2 (2010): 416-43